We are IntechOpen, the world's leading publisher of Open Access books Built by scientists, for scientists

4,800
Open access books available

122,000
International authors and editors

135M
Downloads

Our authors are among the

154
Countries delivered to

TOP 1%
most cited scientists

12.2%
Contributors from top 500 universities

WEB OF SCIENCE™

Selection of our books indexed in the Book Citation Index in Web of Science™ Core Collection (BKCI)

Interested in publishing with us?
Contact book.department@intechopen.com

Numbers displayed above are based on latest data collected.
For more information visit www.intechopen.com

1

Focused Ion Beam Based Three-Dimensional Nano-Machining

Gunasekaran Venugopal[1,2],
Shrikant Saini[1] and Sang-Jae Kim[1,3]
[1]*Jeju National University, Department of Mechanical Engineering, Jeju,*
[2]*Karunya University, Department of Nanosciences and Technology, Tamil Nadu,*
[3]*Jeju National University, Department of Mechatronics Engineering, Jeju,*
[1,3]*South Korea*
[2]*India*

1. Introduction

In recent days, the micro/nano machining becomes an important process to fabricate micro/nano scale dimensional patterns or devices for many applications, especially in electrical and electronic devices. There are two kinds micro-machining in use. i) bulk micro-machining, ii) surface micro-maching. In the case of bulk micromaching, the structures can be made by etching inside a substrate selectively, however, in the case of surface micromachining; the patterns can be made on the top a desired substrate. FIB machining is considered as a one of famous bulk micro-machining processes. Many fabrication methods have been applied to fabricate the devices with smaller sizes (Kim, 1999; Latyshev, 1997). However, conventional until now the size of the smallest pattern was only 2×2 μm^2 was achieved with a lithography technique (Odagawa et al., 1998). Three dimensional as an alternative approach, focused-ion-beam (FIB) etching technique is the best choice for the micro/nano scale patterning. FIB 3-D etching technology is now emerged as an attractive tool for precision lithography. And it is a well recognized technique for making nanoscale stacked-junction devices, nano-ribbons and graphene based 3-D Single Electron Transistor (SET) devices.

FIB micro/nano machining is a direct etching process without the use of masking and process chemicals, and demonstrates sub-micrometer resolution. FIB etching equipments have shown potential for a variety of new applications, in the area of imaging and precision micromachining (Langford, 2001; Seliger, 1979). As a result, the FIB has recently become a popular candidate for fabricating high-quality micro-devices or high-precision microstructures (Melnagilis et al., 1998). For example, in a micro-electro-mechanical system (MEMS), this processing technique produces an ultra microscale structure from a simple sensor device, such as, the Josephson junction to micro-motors (Daniel et al., 1997). Also, the FIB processing enables precise cuts to be made with great flexibility for micro- and nano-technology. Also, the method of fabricating three-dimensional (3-D) micro- and nano-structures on thin films and single crystals by FIB etching have been developed in order to fabricate the 3-D sensor structures (Kim, 2008, 1999).

In this chapter, the focused ion beam (FIB) based three-dimensional nano-machining will be discussed in detail in which the nano-machining procedures are focused with fabricating nanoscale stacked junctions of layered-structured materials such as graphite, $Bi_2Sr_2Ca_{n-1}Cu_nO_{2n+4+x}$ (BSCCO) family superconductor (Bi-2212, Bi-2223, etc.,) and $YBa_2Cu_3O_7$ (YBCO) single crystals, etc. This work could show a potential future in further development of nano-quantum mechanical electron devices and their applications.

2. Classification of machining

Micromachining is the basic technology for fabrication of micro-components of size in the range of 1 to 500 micrometers. Their need arises from miniaturization of various devices in science and engineering, calling for ultra-precision manufacturing and micro-fabrication. Micromachining is used for fabricating micro-channels and micro-grooves in micro-fluidics applications, micro-filters, drug delivery systems, micro-needles, and micro-probes in biotechnology applications. Micro-machined components are crucial for practical advancement in Micro-electromechanical systems (MEMS), Micro-electronics (semiconductor devices and integrated circuit technology) and Nanotechnology. This kind of machining can be applicable for the bulk materials in which the unwanted portions of the materials can be removed while patterning.

In the bulk machining, the materials with the dimensions of more than in the range of micrometer or above centimetre scale are being used for the machining process. A best example for the bulk machining process is that the thread forming process on a screw or bolt, formation of metal components. Also this process can be applicable to produce 3D MEMS structures, which is now being treated as one of older techniques. This also uses anisotropic etching of single crystal silicon. For example, silicon cantilever beam for atomic force microscope (AFM).

Surface micro-machining is another new technique/process for producing MEMS structures. This uses etching techniques to pattern micro-scale structures from polycrystalline (poly) silicon, or metal alloys. Example: accelerometers, pressure sensors, micro gears and transmission, and micro mirrors etc. Micromachining has evolved greatly in the past few decades, to include various techniques, broadly classified into mask-based and tool-based, as depicted in the diagram below.

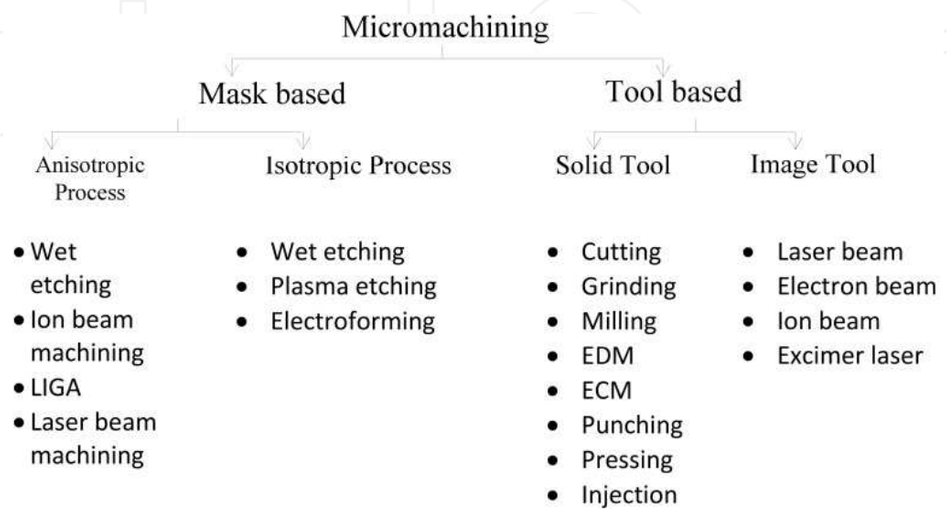

While mask-based processes can generate 2-D/2.5-D features on substrates like semiconductor chips, tools-based processes have the distinct advantage of being able to adapt to metallic and non-metallic surfaces alike, and also generate 3-D features and/or free-form sculpted surfaces. However, the challenges of achieving accuracy, precision and resolution persist.
Internationally, the race to fabricate the smallest possible component has lead to realization of sizes ever below 10 μm, even though the peak industrial requirement has been recognized at 100s of μm. Thus, the present situation is particularly advantageous for the industry that develops/fabricates nano/micron scale components.

2.1 Various techniques of micromachining

Micromachining can be done by following various techniques.

a. Photolithography
b. Etching
c. LIGA
d. Laser Ablation
e. Mechanical micromachining

Photolithography

This technique is being used in microelectronics fabrication and also used to pattern oxide/nitride/polysilicon films on silicon substrate. In this process, the basic steps involved are, photoresist development, etching, and resist removal. Photolithographic process can be described as follows:
The wafers are chemically cleaned to remove particulate matter, organic, ionic, and metallic impurities. High-speed centrifugal whirling of silicon wafers known as "Spin Coating" produces a thin uniform layer of photoresist (a light sensitive polymer) on the wafers. Photoresist is exposed to a set of lights through a mask often made of quartz. Wavelength of light ranges from 300-500 nm (UV) and X-rays (wavelengths 4-50 Angstroms). Two types of photoresist are used: (a) Positive: whatever shows, goes (b) Negative: whatever shows, stays. The photo resist characteristics after UV exposure are shown below in Fig. 1

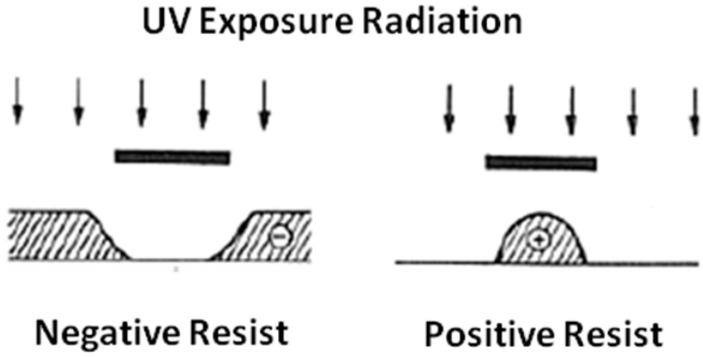

Fig. 1. Photoresist characteristics in UV exposure

Etching

Normally etching process can be classified in to two kinds. (a) Wet etching (b) Dry etching.
The wet etching process involves transport of reactants to the surface, surface reaction and transport of products from surfaces. The key ingredients are the oxidizer (e.g. H_2O_2, HNO_3),

the acid or base to dissolve the oxidized surface (e.g. H_2SO_4, NH_4OH) and dilutent media to transport the products through (e.g. H_2O). Dry etching process involves two kinds. (a) plasma based and (b) non plasma based.

LIGA

The LIGA is a German term which means LIthographie (Lithography) **G**alvanoformung (Electroforming) **A**bforming (Molding). The exact English meaning of LIGA is given in parenthesis. This process involves X-ray irradiation, resist development, electroforming and resist removal.

The detailed LIGA process description is discussed below:

- Deep X-ray lithography and mask technology
  - Deep X-ray (0.01 – 1nm wavelength) lithography can produce high aspect ratios (1 mm high and a lateral resolution of 0.2 µm).
  - X-rays break chemical bonds in the resist; exposed resist is dissolved using wet-etching process.
- Electroforming
  - The spaces generated by the removal of the irradiated plastic material are filled with metal (e.g. Ni) using electro-deposition process.
  - Precision grinding with diamond slurry-based metal plate used to remove substrate layer/metal layer.
- Resist Removal
  - PMMA resist exposed to X-ray and removed by exposure to oxygen plasma or through wet-etching.
- Plastic Molding
  - Metal mold from LIGA used for injection molding of MEMS.

LIGA Process Capability

- High aspect ratio structures: 10-50 µm with Max. height of 1-500 µm
- Surface roughness < 50 nm
- High accuracy < 1µm

Laser ablation

High-power laser pulses are used to evaporate matter from a target surface. In this process, a supersonic jet of particles (plume) is ejected normal to the target surface which condenses on substrate opposite to target. The ablation process takes place in a vacuum chamber - either in vacuum or in the presence of some background gas. The graphical process scheme is given below in Fig.2.

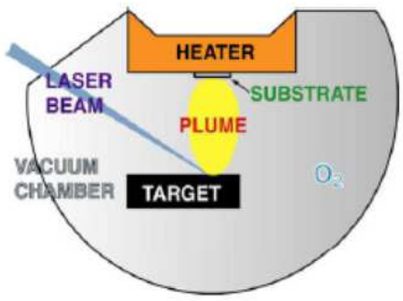

Fig. 2. Laser ablation experiment.

Mechanical micromachining

Lithography or etching methods are not capable of making true 3D structures e.g. free form surfaces and also limited in range of materials. Mechanical machining is capable of making free form surfaces in wide range of materials. Can we scale conventional/non-traditional machining processes down to the micron level? Yes! There are two approaches used to machine micron and sub-micron scale features.

1. Design ultra precision (nanometer positioning resolution) machine tools and cutting tools. For this, ultra precision diamond turning machines can be used.
2. Design miniature but precise machine tools
   Example: Micro-lathe, micro-mill, micro-EDM, etc

Mechanical micromachining process descriptions are given below:

- Can produce extremely smooth, precise, high resolution true 3D structures
- Expensive, non-parallel, but handles much larger substrates
- Precision cutting on lathes produces miniature screws, etc with 12 μm accuracy
- Relative tolerances are typically 1/10 to 1/1000 of feature
- Absolute tolerances are typically similar to those for conventional precision machining (Micrometer to sub-micrometer)

2.2 Focused-ion-beam (FIB) technique for nanofabrication

The focused ion beam based nanofabrication method can be followed for the fabricating the nanoscale devices on materials based on metal and non-metallic elements, particularly the layered structure materials like graphite, Bi-2212 and YBCO which are recently attracted the world scientific community due to their interesting electrical and electronic properties reported in recent reports (Venugopal, 2011; Kim, 2001).

Graphite is considered as a well known layered-structured material in which carbon sheets are arranged in a stacked-manner with interlayer distance of 0.34 nm. Each single graphite sheet is known as a graphene layer which is now becoming as one of hot topic in the world scientific community. In the recent reports (Venugopal, 2011a, 2011b, 2011c), the fabrication of submicron and below submicron stacked junctions were carved from the bulk graphite materials using FIB 3-D etching. The interesting results were obtained in those observations that the graphite stacked-junction with in-plane area A of 0.25 μm² showed nonlinear concave-like I–V characteristics even at 300 K; however the stack with A ≥ 1 μm² were shown an ohmic-like I–V characteristic at 300 K for both low and high-current biasing. It turned into nonlinear characteristics when the temperature goes down. These results may open road to develop further graphite based nonlinear electronic devices. Further researches are being carried out to find unexplored properties of graphite nano devices fabricated using FIB micro/nano machining technology.

The focused ion beam (FIB) machining to make micro-devices and microstructures has gained more and more attention recently (Tseng, 2004). FIB can be used as a direct milling method to make microstructures without involving complicated masks and pattern transfer processes. FIB machining has advantages of high feature resolution, and imposes no limitations on fabrication materials and geometry. Focused ion beams operate in the range of 10-200 keV. As the ions penetrate the material, they loose their energy and remove substrate atoms. FIB has proven to be an essential tool for highly localized implantation doping, mixing, micromachining, controlled damage as well as ion-induced deposition. The technological challenge to fabricate nanoholes using electron beam lithography and the

minimal feature size accessible by these techniques is typically limited to tens of nanometers, thus novel procedures must be devised (Zhou, 2006).

The patterning of samples using the FIB (focused ion beam) technique is a very popular technique in the field of inspection of integrated circuits and electronic devices manufactured by the semi-conductor industry or research laboratories. This is the case mainly for prototyping devices. The FIB technique allowing us to engrave materials at very low dimensions is a complement of usual lithographic techniques such as optical lithography. The main difference is that FIB allows direct patterning and therefore does not require an intermediate sensitive media or process (resist, metal deposited film, etching process). FIB allows 3D patterning of target materials using a finely focused pencil of ions having speeds of several hundreds of km s^{-1} at impact. Concerning the nature of the ions most existing metals can be used in FIB technology as pure elements or in the form of alloys, although gallium (Ga^+ ions) is preferred in most cases.

Many device fabrication techniques based on electron beam lithography followed by reactive-ion etching (RIE), chemical methods, and evaporation using hard Si shadow masks, and including lithography-free fabrication, have been reported. The procedures, however, are complex and yield devices with dimensions of ~5 to 50 nm, which are restricted to simple geometries. RIE creates disordered edges, and the chemical methods produce irregular shapes with distributed flakes, which are not suitable for electronic-device application.

Practically, FIB patterning can be achieved either by local surface defect generation, by ion implantation or by local sputtering. These adjustments are obtained very easily by varying the locally deposited ion fluence with reference to the sensitivity of the target and to the selected FIB processing method (Gierak, 2009). The FIB milling involves two processes: 1) Sputtering, ions with high energy displace and remove atoms of substrate material, and the ions lose their energy as they go into the substrate; 2) Re-deposition, the displaced substrate atoms, that have gained energy from ions through energy transfer, go through similar process as ions, sputtering other atoms, taking their vacancy, or flying out.

A focused gallium ion beam having an energy typically around 30 keV is scanned over the sample surface to create a pattern through topographical modification, deposition or sputtering. A first consequence is that, mainly because of the high ion doses required (~10^{18} ions cm^{-2}) and of the limited beam particle intensity available in the probe, FIB etching-based processes remain relatively slow. We may recall that for most materials, the material removal rate for 30 keV gallium ions is around 1–10 atoms per incident ion, corresponding to a machining rate of around 0.1–1 μm^3 per nC of incident ions (Gierak, 2009). The second consequence is that for most applications the spatial extension of the phenomena induced by focused ion beam irradiation constitutes a major drawback.

In addition, there have been few reports of the fabrication of nano-structured materials, nano devices, and hierarchical nano-sized patterns with a 100 nm distance using a focused ion beam (FIB). Fabrication of graphene nanoribbons and graphene-based ultracapacitors were also reported recently. The above-discussed methods were followed by the two-dimensional (2D) fabrication methods and required extensive efforts to achieve precise control. Hence, a novel three-dimensional (3D) nanoscale approach to the fabrication of a stack of graphene layers via FIB etching is proposed, through which a thin graphite flake can be etched in the *c*-axis direction (stack height with a few tens of nanometers). Also the main purpose of describing graphite and other BSCCO based superconducting nanoscale devices is that these layered structured materials have shown an excellent device structures

during fabrication and their electrical transport characteristics were interesting which will be useful to future works.

2.2.1 Nanoscale stack fabrication by focused-ion-beam

Using an FIB, perfect stacks can be fabricated more easily along the c-axis in thin films and single-crystal whiskers. FIB 3D etching has been recognized as a well-known method for fabricating high-precision ultra-small devices, in which etching is a direct milling process that does not involve the use of any masking and process chemicals and that demonstrates a submicrometer resolution. Thus, these our proposal is focused on the fabrication of a nanoscale stack from the layered structured materials like thin graphite flake and BSCCO, via FIB 3D etching. The detailed schematic of fabrication process is shown in Fig. 3.

The 3D etching technique is followed by tilting the substrate stage up to 90° automatically for etching thin graphite flake. We have freedom to tilt the substrate stage up to 60° and rotate up to 360°. To achieve our goal, we used sample stage that itself inclined by 60° with respect to the direction of the ion beam (fig 3a). The lateral dimensions of the sample were 0.5×0.5 μm². The in-plane area was defined by tilting the sample stage by 30° anticlockwise with respect to the ion beam and milling along the *ab*-plane.

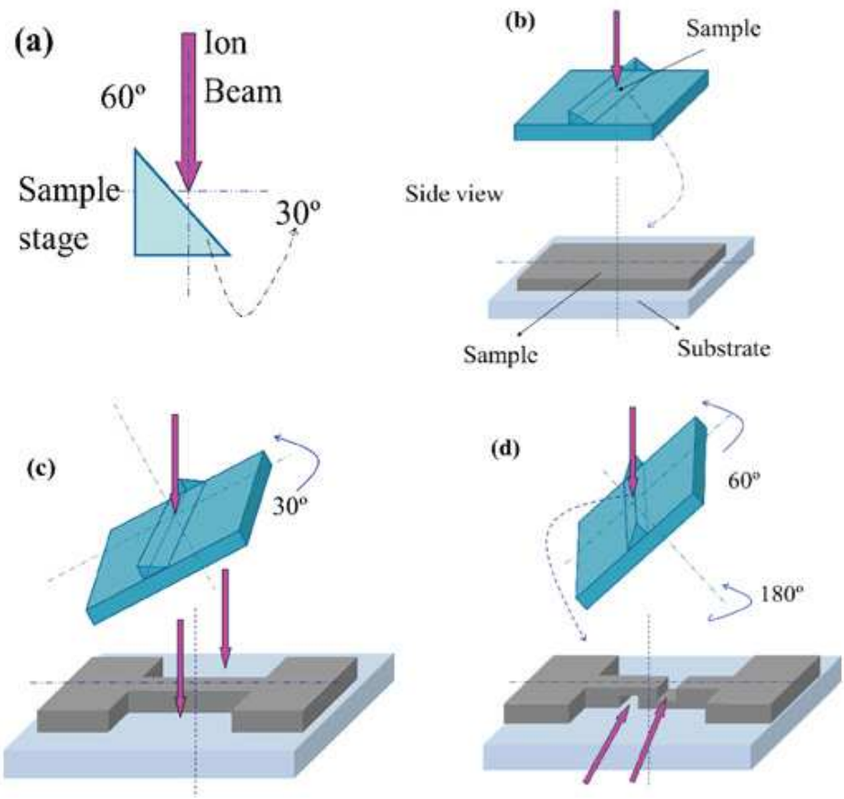

Fig. 3. FIB 3-D fabrication process (a) Scheme of the inclined plane has an angle of 60° with ion beam (where we mount sample). (b) The initial orientation of sample and sample stage. (c) Sample stage titled by 30° anticlockwise with respect to ion beam and milling along ab-plane. (d) The sample stage rotated by an angle of 180° and also tilted by 60° anticlockwise with respect to ion beam and milled along the c-axis.

The in-plane etching process is shown in Fig. 3(a)–(c). The out of plane or the c-axis plane was fabricated by rotating the sample stage by an angle of 180°, then tilting by 60° anticlockwise with respect to the ion beam, and milling along the c-axis direction. The schematic diagram of the fabrication process for the side-plane is shown in Fig. 3(d). The dimensions of the side-plane was W=0.5 µm, L=0.5 µm, and H=200 nm. The c-axis height length (H) of the stack was set as 200 nm. An FIB image of fabricated stack is shown in Fig. 4 in which the schematic of stack arrangement (graphene layers with interlayer distance 0.34 nm) was also shown in the inset (top right) in Fig. 4. The vertical red arrow indicates the current flow direction through the stack.

2.2.2 Transport characteristics of nanoscale graphite stacks

The electrical transport characteristics (including ρ-T and I-V) can be performed for the fabricated stack using closed-cycle refrigerator systems (CKW-21, Sumitomo) at various temperatures from 25 to 300 K with the use of the Keithley 2182A nanovoltmeters and AC & DC current source (6221). The I-V characteristics of the fabricated stack are shown in Fig.4.

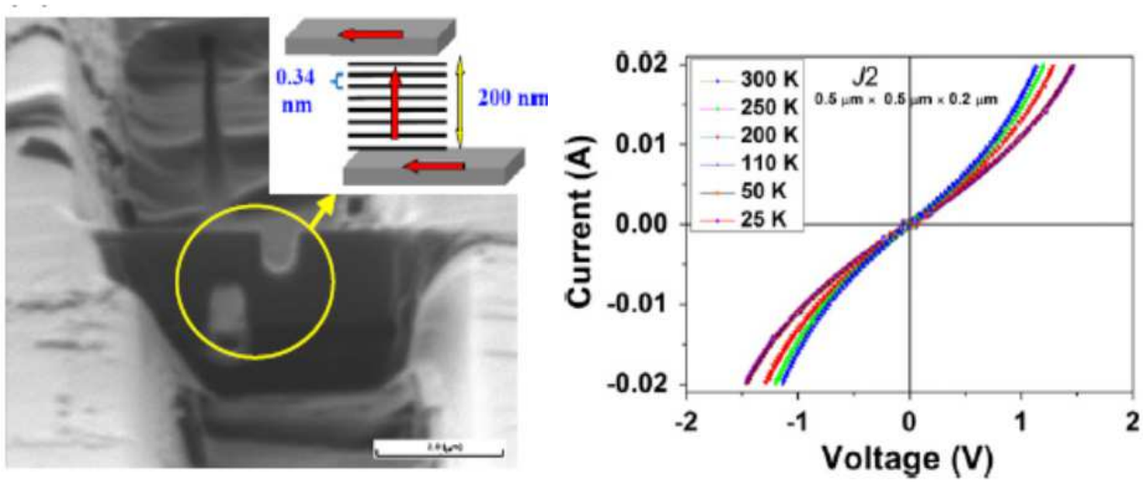

Fig. 4. FIB image of the nanoscale stack fabricated on a thin graphite flake along the c-axis height of 200 nm (image scale bar is 2 µm). Inset shows the schematic diagram of stack arrangement along the c-axis. (Venugopal et al, 2011). The vertical red arrow indicates the current flow direction through the nanoscale stack. I-V characteristics at various temperatures of the fabricated nanostack are also shown (right).

The FIB ion damage effect can be avoided if the device is fabricated at a 3D angle, in which the top layer of *ab*-plane will act as a masking layer and the ion beam is exactly perpendicular to the milling surface. The expected ion damage effect was simulated using the TRIM software (Ziegler, 1996) and the fabrication parameter of etching process for the 30 keV Ga^+ ions was optimized. It was found from the simulation results that the depth of ion implantation is consistent with 10 nm. Majority (>95%) of the Ga^+ ions are expected to be implanted within 10 nm of the side walls of stack surface, with a much smaller fraction, eventually stopping at as deep as 10 nm into the surface. Therefore, the proportion of the fabricated stack affected by ion beam damage is not very large, and it does not affect the quality of graphite devices in the *c*-axis direction.

By varying in-plane area (*A*) and stack height (*H*), several stacked-junctions with the dimensions of W = 1 μm, L = 1 μm, and H = 0.1 μm (denoted as *J4*) and W = 2 μm, L = 1 μm, and H = 0.3 μm (denoted as *J5*) were fabricated. The electrical transport characteristics were performed for these stacks and compared their results. The current-voltage (*I-V*) characteristics of the nanostack with in-plane area (*A)* of 0.25 μm^2 (*J*2) at various temperatures, are presented in Fig. 4. The stack showed a nonlinear concave-like *I-V* characteristics at all studied temperatures (25, 50, 110, 200, 250 and 300 K). At 300 K, the stack resistance was found as 75 Ω. The stack resistance found increases when the temperature goes down to 25 K.

The electrical characteristics of nanostack (*J*2) were analyzed and compared with bigger junctions *J4* (1 × 1 × 0.1 μm^3) and *J5* (2 × 1 × 0.3 μm^3). From the data analysis, it is clear that the stack with larger height and reduced in-plane effective area (*A*) has shown higher resistance than the stack with larger in-plane area (*A*). The *I-V* characteristics of junctions *J*4 and *J*5 at different temperatures are shown in Fig. 5 (a) and (b) respectively. A typical *c*-axis transport characteristics similar to junction *J*2 was observed. However the nonlinear *I-V* characteristics were not observed at 300 K, but ohmic like-linear behavior is observed. When the temperature goes down, this behavior is turned into curve-like nonlinear characteristics.

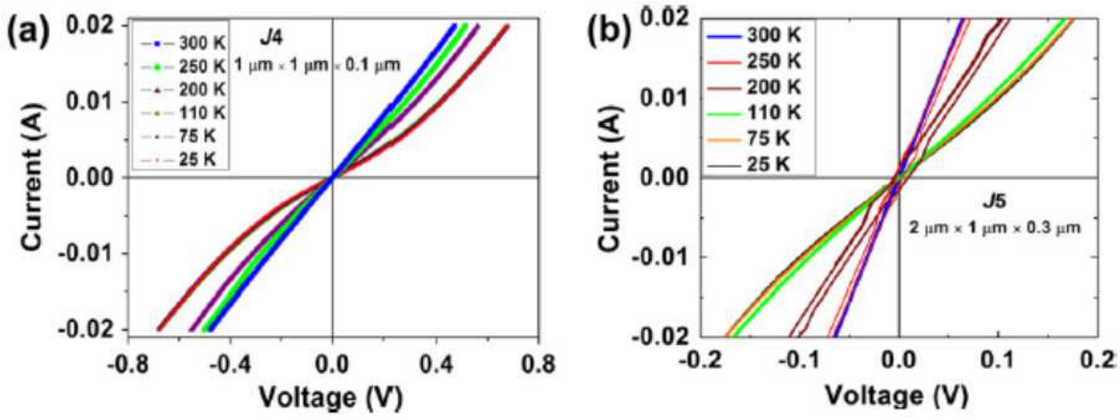

Fig. 5. (a) I–V characteristics of a bigger stacked-junction with A of 1 μm^2 (J4) at different temperature from 25 K to 300 K. (b) I–V characteristics of another bigger junction with A of 2 × 1 × 0.3 μm^3 (J5) at different temperature from 25 K to 300 K. Both the junctions show ohmic like behavior at 300 K; however the same behavior turned into nonlinear characteristics when the temperature goes down (Venugopal et al, 2011).

There is a significant overlap of *I-V* curves for temperatures 110, 75 and 25 K. For graphite stacks with $A \geq 1$ μm^2, there was no nonlinear *I-V* characteristics observed at 300 K even at high biasing. With a decrease of the stack size down to 0.25 μm^2, the junction shows clear nonlinear concave-like *I-V* characteristics for both 300 K and 25 K. Since the fabricated stack contains multiple elementary junctions along the *c*-axis, the nonlinear concave-like tunneling characteristics appeared from the *I-V* characteristics (Venugopal et al, 2011).

2.2.3 Temperature dependent resistivity of nanoscale graphite stack

Fig 6 represents the ρ–T characteristics of stacked-junction (J2). The junction J2 shows a semiconducting behavior for T > 65 K and metallic characteristics for T < 65 K. Above 65 K,

thermal excitation of carriers plays a major role in semiconducting temperature dependence. However below 65 K, the interlayer hopping conduction combined with scattering of carriers by phonons can be responsible for the metallic-like temperature dependence. The ρ–T characteristics along the *ab*-plane transport are shown as inset in Fig. 6. A well understood metallic behavior was observed. This behavior is well agreed with earlier observations on c-axis characteristics of bulk graphite material (Matsubara, 1990).

An electron motion parallel to its plane is not affected by the stacking faults, however, but an electron motion in the *c*-axis direction is strongly impeded by the faults. The combined effects of impurity-assisted hopping, tunneling current, and the thermal excitation of the carriers on the plane of a stack play important roles in this temperature-dependent conduction mechanism in layered structured materials such as graphite.

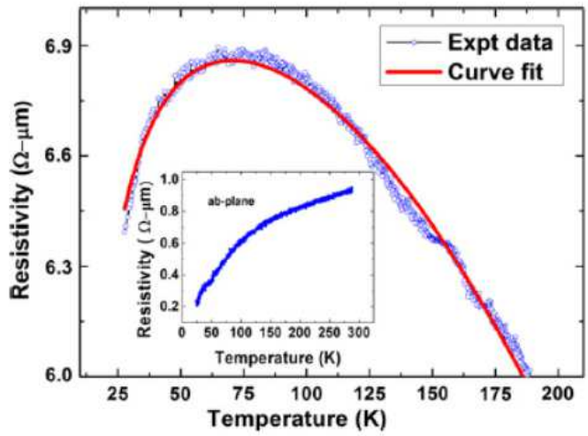

Fig. 6. The resistivity–temperature (ρ-T) characteristics of nanostack which shows a clear c-axis characteristics of graphite. A well agreed curve fitting to experimental data is also shown. A clear metallic behavior is observed for *ab*-plane transport of bare graphite flake which is shown as inset. (Venugopal, 2011)

2.3 FIB nano fabrication on superconducting devices

Considering Bi-family as a layered structure material, there are three compounds in the Bi-family high-temperature superconductors, differing in the type of planar CuO_2 layers; single-layered $Bi_2Sr_2CuO_{6+\delta}$ (Bi-2201) single crystal, double-layered $Bi_2Sr_2CaCu_2O_{8+\delta}$ (Bi-2212) single crystal, and triple-layered $Bi_2Sr_2Ca_2Cu_3O_{10+\delta}$ (Bi-2223) single crystal (Saini, 2010). This Bi-family material is a one of the famous emerging material for electron tunneling devices, such as intrinsic Josephson junctions (IJJ) in layered high-*Tc* superconductors. The spacing of consecutive copper-oxide double planes in the most anisotropic cuprate superconductors is greater than the coherence length in the out-of-plane *c*-direction. When a current flows along the *c*-direction in such a material, it therefore flows through a series array of "intrinsic" Josephson junctions (IJJs) (Kleiner, 1992). These junctions and junction arrays are showing promise for a wide variety of applications, including as voltage standards and sub-mm-wave oscillators (Wang, 2001). For sub-micron intrinsic junctions, there is an additional range of potential applications exploiting the Coulomb blockade effect, when the E_c is charging energy $E_c \geq E_J$, K_BT, where E_J is the Josephson energy & k_BT is thermal energy. These applications include electric-field sensors

and quantum current standards (Bylander, 2005). In long arrays of junctions, E_c is enhanced by electron-electron interactions (Likharev, 1989, 1995) by a factor $[C/C_0]^{1/2}$, where C is the junction capacitance and C_0 is the stray capacitance to ground. The large ratio $C/C_0 \sim 10^6$ for intrinsic junctions makes them particularly suited to the applications involving Coulomb blockade effects. The features of the single Cooper-pair tunneling effect from the layered structure of Bi-family as well as for YBCO will also be discussed in detail.

Superconductivity is a phenomenon when the resistance of the material becomes zero and it expels all the magnetic field below a certain temperature usually at very low temperature. The phenomenon of superconductivity was discovered in 1911 by the Dutch physicist H. Kamerlingh Onnes. The quantum application of superconductivity was introduced in 1962. B. D. Josephson discovered a tunnel junction consists of two strips of superconductors separated by an insulator where the insulator is so thin that electrons can tunnel through it known as Josephson junction.

The schematic of different types of Josephson junctions are shown below in Fig.7. S stands for superconductor, S′ for a superconductor above T_c, N for normal metal, Se for semiconductor, and I for an insulator.

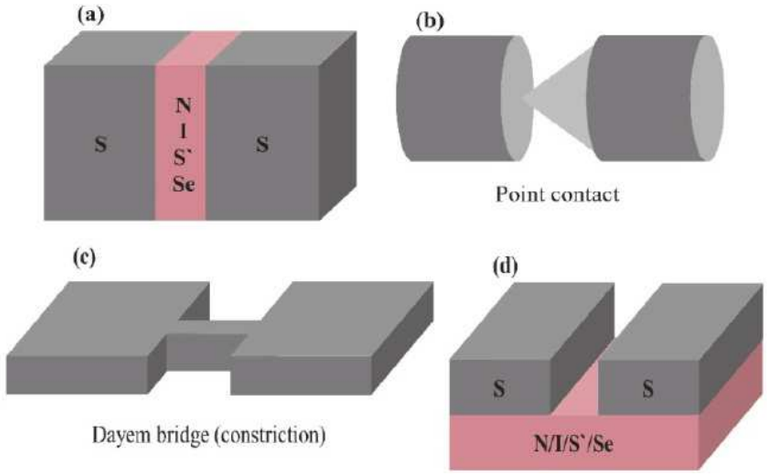

Fig. 7. The schematics of different types of superconducting devices.

The term high-temperature superconductor was first introduced in 1986 to designate the new family of cuprate-perovskite ceramic materials discovered by Johannes George Bednorz and Karl Alexander Müller [J. G. Bednorz, K. A. Mueller (1986) "Possible high T_C superconductivity in the Ba-La-Cu-O system", *Zeitschrift für Physik B* 64 (2) 189–193 doi:10.1007/BF01303701] for which they won the Nobel Prize in Physics in the following year. Their discovery of the first high-temperature superconductor, LaBaCuO, with a transition temperature of 30 K, generated great excitement. In 1988, BSCCO ($Bi_2Sr_2Ca_{n-1}Cu_nO_{2n+4+x}$, with n=2 being the most commonly studied compound, though n=1 and n=3 have also received significant attention) as a new class of superconductor was discovered by Maeda and coworkers [H. Maeda, Y. Tanaka, M. Fukutumi, and T. Asano (1988) "A New High-T_c Oxide Superconductor without a Rare Earth Element" *Jpn. J. Appl. Phys.* 27 (2) L209–L210. doi:10.1143/JJAP.27.L209.] at the National Research Institute for Metals in Japan, though at the time they were unable to determine its precise composition and structure. The discovery of these high temperature superconductors gave a path for the application of the superconductivity at higher temperature.

2.3.1 FIB nanomachining of Intrinsic Josephson Junctions (IJJs) on BSCCO and Y123/Pr123 multilayered thin films

Many fabrication methods based on high-resolution patterning have been applied to develop high-*Tc* superconducting devices. Very small structures are needed in the fabrication of tunneling devices, such as intrinsic Josephson junctions (IJJ) in layered high *Tc* superconductors $Bi_2Sr_2CaCu_2O_{8+\delta}$ (Bi-2212). Perfect stacks are more easily obtained in *c*-axis high-quality thin films than in *a*-axis films or single-crystal whiskers. However, the IJJ fabrication process using *c*-axis thin films and single crystals requires intricate processes and limits the junction size in mesa structures.

As per previous reports, the fabrication of IJJs by the focused ion beam (FIB) etching method using single-crystal whiskers as a base material requires some complicated processes, including turning over of the sample. As an alternative approach, in this chapter, a three-dimensional IJJ fabrication method is presented using *c*-axis thin films. The fabrication steps using *c*-axis single crystal are also simplified by the *in situ* process. Here, the 3D FIB etching methods using YBCO thin films and Bi-2212 single-crystal whiskers were described as examples with a successive decrease of their in-plane area, *S*, down to a submicron scale. Also, there was a possibility to identify the features of the single Cooper-pair tunneling effect from the layered structure of Bi-2212 with very narrow interval between layers.

FIB image of a submicron stack fabricated on Bi-2212 single crystal whiskers with in-plane area of 0.4 μm × 0.4 μm and schematic of the IJJs configuration are shown in Fig. 8, in which FIB fabrication procedures followed as described in section 2.1.2.

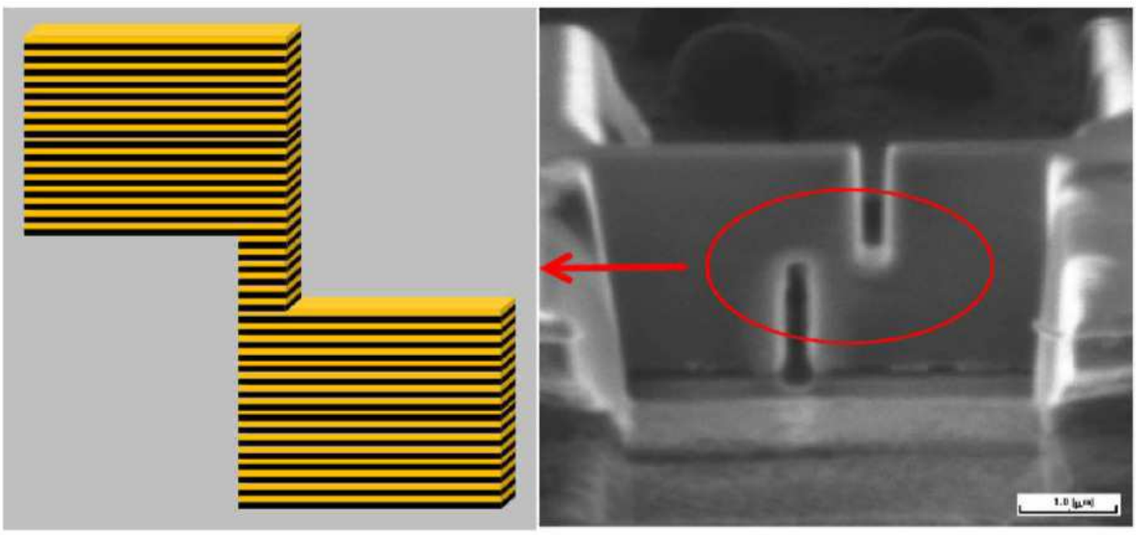

Fig. 8. FIB image of a submicron stack fabricated on Bi-2212 single crystal whisker. The red color circular part shown in stack contains many IJJs.

FIB image of submicron stack (scale bar of 1 μm) and schematic of the Josephson junctions configuration in the submicron stack fabricated on *a*-axis oriented $YBa_2Cu_3O_7/PrBa_2Cu_3O_7$ multi layered thin films are shown in Fig.9. The arrow indicates the direction of current to observe the effect of Josephson junctions. The axial direction of thin film is shown in the expended view.

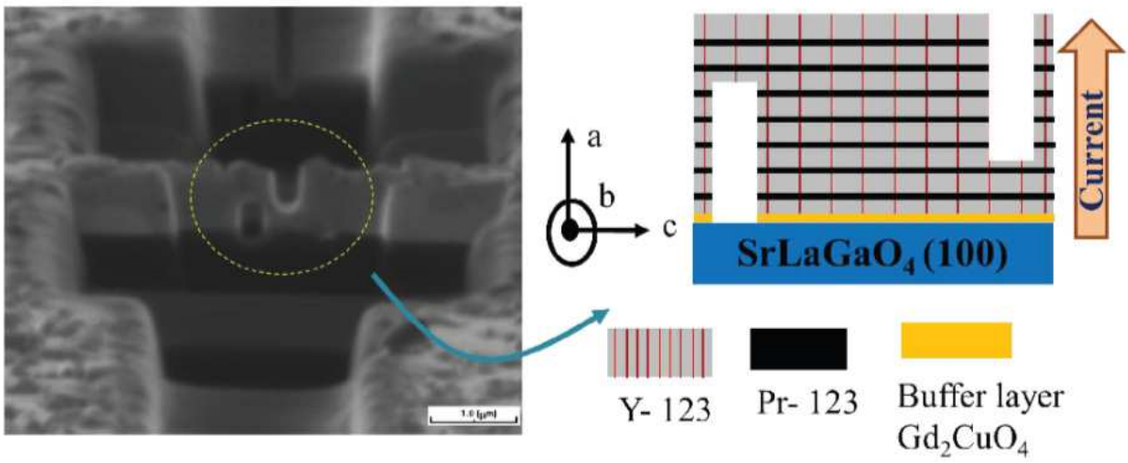

Fig. 9. FIB image of a submicron stack fabricated on *a*-axis oriented Y123/Pr123 multi layered thin films.

2.3.2 Electrical transport characteristics of Josephson junctions fabricated on multi layered thin films of Y123/Pr123

Fig. 10 represents *R-T* characteristics of the Josephson junctions fabricated on multi layered thin films of Y123/Pr123 which shows T_c about 83 K.

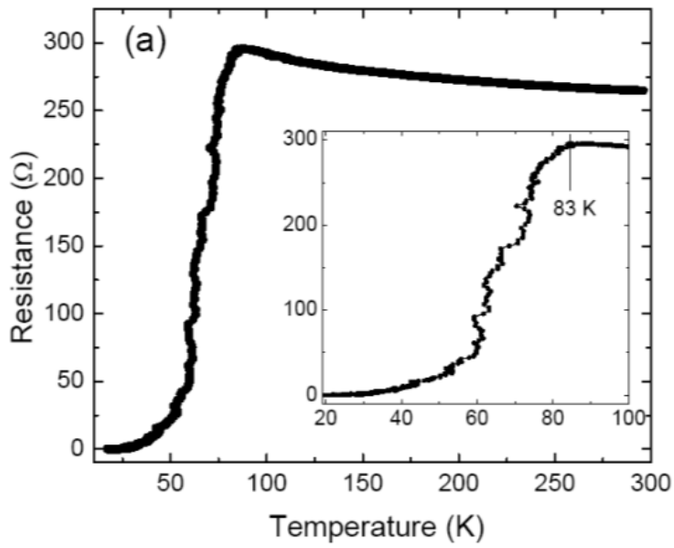

Fig. 10. *R-T* characteristics of the device show T_c about 83 K.

I-V characteristics of the same device were studied without microwave irradiation at different temperature of 10, 20, and 30 K, shown in Fig. 11. As temperature decreases, the critical current density of superconducting device is increases gradually.

The above discussed nanomachining/milling techniques followed by focused ion beam 3-D technique shall be applicable to other layered-structured materials rather than graphite flake, BSCCO, YBCO and multilayered thin films, etc,. This may have great potential in future nanodevice development and applications.

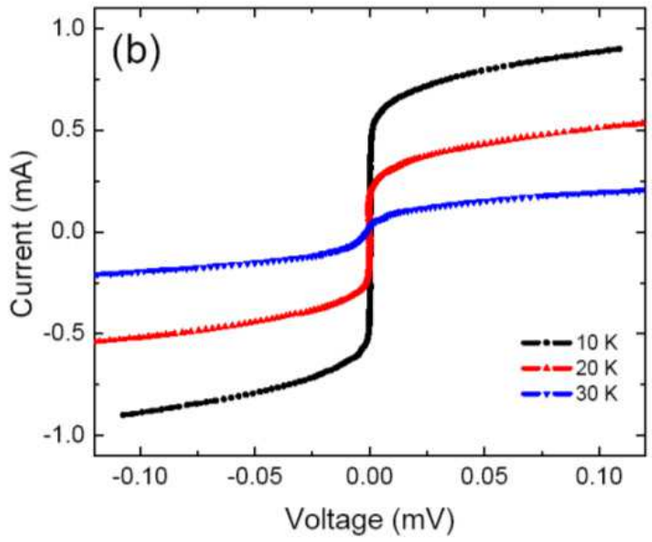

Fig. 11. *I-V* characteristics of the device without microwave irradiation at different temperature of 10, 20, and 30 K. The critical current density J_c about 2.2 X 10^5 A/cm^2 is measured at 20 K.

2.4 Future advances

In the future, micromachining is destined to improve upon its shortcomings, as the various micromachining processes become accurate, reliable, versatile and cost-effective. In India, BARC has established premier micromachining and nano-finishing facilities along with state-of-the art metrology systems. On the other hand, IIT Bombay has also taken a lead in establishing tool-based micromachining facilities. Even at South Korea, the technology towards nanomachining becomes popular nowadays and the active research is now under progress through which an interesting studies may be explored in near future.

FIB technology is still relatively young compared with other semiconductor fabrication processes. One of the major challenges for all of the microfabrication and nanofabrication technologies is to downscale the feature size while maintaining a high throughput. To increase the throughput and the ability to be used in production, the milling rate of the existing FIB milling systems has to be improved. A variable-diameter beam system should be developed to provide multi-resolution milling to cope with different accuracy or tolerance requirements. It is ideal that the beam diameter can be continuously changed in situ. (Tseng, 2004). This type of system has been available for many macro-scale fabrication processes. With this system, a larger beam can be used for roughing 'cut' (milling) to increase the milling rate in regions where only lower resolution is needed. The advantages to use a heavy-duty two-lens system with improved automation should be examined with the goal to develop a system for limited production usage first. Once the high-performance FIB system is used in production, it can be a vital candidate to become the mainstream tool for the future microtechnology and nanotechnology industry.

With an increasing awareness about the advantages of manufacturing micro-components indigenously instead of importing at high costs, the researchers and industrialists are in need of the knowledge of micromachining technology.

3. Conclusion

In conclusion, the focused ion beam based nanomachining have been discussed in detail for the layered structured materials, BSCCO superconducting devices, YBCO based thin film devices, and a-axis oriented Y123/Pr123 multi layered thin film devices. The development of focused ion beam technology based nanomachining is one amongst many examples on how research results may have found unexpected applications in totally different application areas. This is particularly true for the FIB technology development itself that has benefited from all the previously made advances in field emission physics, charged particle optics theory or modelling and in fundamental instrumentation or applied metrology. All these advances were very quickly and efficiently integrated into FIB instruments, so that in less than one decade FIB instruments have moved out from some specialist laboratories to enter almost every modern laboratory, research institute or processing environment. This is also true for the semiconductor industry that has been almost immediately applying FIB systems for device inspection failure analysis and reverse engineering with roaring success.
The FIB processing methods which we discussed in this chapter, appear now to be well suited and very promising for several diverse nanotechnology applications, and may be of major interest for future applications to spin-electronics, nano-electronics, nano-optics or nanomagnetism.

4. Acknowledgment

This research was supported by National Research Foundation of Korea Grant under contract numbers 2009-0087091 and 2011-0015829 through the Human Resource Training Project for Regional Innovation. A part of this research was also supported by the 2012 Jeju Sea Grant College Program funded by Ministry of Land, Transport and Maritime Affairs, Republic of Korea

5. References

Bylander, J. (2005). Current Measurement by Real-time Counting of Single Electrons.. *Nature.*, Vol.434, pp. 361-364.

Daniel, J. H. (1997). Focused Ion Beams in Microsystem Fabrication. M*icroelectron. Eng.*, Vol.35, No.1-4, pp. 431-434.

Gierak, J. (2009). Focused Ion Beam Technology and Ultimate Applications. *Semicond. Sci. Technol.*, Vol.24, pp. 043001-043022.

Kim, S. J. (2001). Fabrication and Characteristics of Submicron Tunnelling Junctions on High Tc Superconducting c-axis Thin Films and Single Crystals. *J. Appl. Phys.*, Vol.89, No.11, pp. 7675-7677.

Kim, S. J. (1999). Submicron Stacked-junction Fabrication from $Bi_2Sr_2CaCu_2O_{8+\delta}$ Whiskers by Focused-Ion-Beam Etching . *Appl. Phys. Lett.*, Vol.74, No.8, pp. 1156-1158.

Kim, S. J. (2008). Development of Focused Ion Beam Machining Systems for Fabricating Three-dimensional Structures. *Jpn. J. Appl. Phys.*, Vol.47, No.6, pp. 5120-5122.

Kim, S. J. (1999). 3D intrinsic Josephson junctions using c-axis thin films and single crystals. *Supercond. Sci. Technol.*, Vol.12, pp. 729-731.

Kleiner, R. (1992). Intrinsic Josephson Effects in BiSrCaCuO Single-Crystals. *Phys. Rev. Lett.*, Vol.68, pp. 2394-2396.

Latyshev, Y. I. (1997). Intrinsic Josephson Effects on Stacks Fabricated from High Quality BSCCO 2212 Single Crystal Whiskers. *Physica C.,* Vol.293, pp. 174-180.

Langford, R. M. (2001). Preparation of Site Specific Transmission Electron Microscopy Plan-view Specimens using a Focused Ion Beam System. *J. Vac. Sci. Technol. B.,* Vol.19, No.755. doi:10.1116/1.1371317.

Likharev, K. K. (1989). Single-electron Tunnel Junction Array: An Electrostatic Anolog of the Josephson Transmission Line. *IEEE Trans. Mag.,* Vol.25, pp. 1436. DOI: 10.1109/20.92566.

Likharev, K. K. (1995). Electron-electron Interaction in Linear Arays of Small Tunnel Junctions. *Appl. Phys. Lett.,* Vol.67, pp. 3037-3039.

Matsubara, K. (1990). Electrical Resistance in c-direction of Graphite. *Phys. Rev. B.,* Vol.41, pp. 969-974.

Melnagilis, J. (1998). A Review of Ion Projection Lithography. *J. Vac. Sci. Technol. B.,* Vol.16, No.3, pp. 927-957.

Odagawa, A. (1998). Characteristics of Intrinsic Josephson Junctions in Thin Stack on Bi-2223 Thin Films. *Jpn. J. Appl. Phys.,* Vol.37, No.1, pp. 486-491.

Saini, S. (2010). Characterization of Submicron Sized Josephson Junction Fabricated in a $Bi_2Sr_2Ca_2Cu_3O_{10+\delta}$ (Bi-2223) Single Crystal Whisker. *J. Supercond. Nov. Magn.* Vol.23, pp. 811-813.

Seliger, R. L. (1979). High-resolution, Ion-beam Processes for Microstructure Fabrication. *J. Vac. Sci. Technol. B.,* Vol.16, No.6, pp.1610-1612.

Tseng, A. A. (2004). Recent Developments in Micromilling using Focused Ion Beam Technology. *J. Micromech. Microengg.,* Vol.14, pp. R15-R34.

Venugopal, G. (2011a). Fabrication of Nanoscale Three-dimensional Graphite Stacked-junctions by Focused-ion-beam and Observation of Anomalous Transport Characteristics. *Carbon,* Vol.49, No.8, pp. 2766-2772.

Venugopal, G. (2011b). Temperature Dependence of Transport Anisotrophy of Planar-type Graphite Nano-structures Fabricated by Focused Ion Beam. *J. Nanosci. Nanotechnol.* Vol.11, No.1, pp. 296-300.

Venugopal, G. (2011c). Fabrication and Characteristics of Submicron Stacked-Junctions on Thin Graphite Flakes. *J. Nanosci. Nanotechnol*. Vol.11, No.2, pp. 1405-1408.

Wang, H. B. (2001). Terahertz Responses of Intrinsic Josephson Junctions in High Tc Superconductors. *Phys. Rev. Lett.,* Vol.87, pp. 107002-107005.

Ziegler, J. F; Biersack, J. P. & Littmark, U. (1996). *The Stopping and Range of Ions in Solids,* Pergamon, New York.

Zhou, J.; Yang, G. (2006). *Proceedings of the 7th ICFDM 2006 International Conference on Frontiers of Design and Manufacturing,* pp. 453-458, Guangzhou, China, June 19-22, 2006

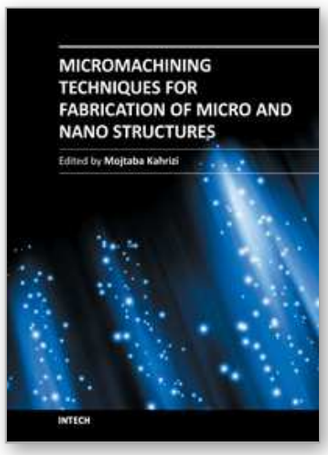

Micromachining Techniques for Fabrication of Micro and Nano Structures

Edited by Dr. Mojtaba Kahrizi

ISBN 978-953-307-906-6
Hard cover, 300 pages
Publisher InTech
Published online 03, February, 2012
Published in print edition February, 2012

Micromachining is used to fabricate three-dimensional microstructures and it is the foundation of a technology called Micro-Electro-Mechanical-Systems (MEMS). Bulk micromachining and surface micromachining are two major categories (among others) in this field. This book presents advances in micromachining technology. For this, we have gathered review articles related to various techniques and methods of micro/nano fabrications, like focused ion beams, laser ablation, and several other specialized techniques, from esteemed researchers and scientists around the world. Each chapter gives a complete description of a specific micromachining method, design, associate analytical works, experimental set-up, and the final fabricated devices, followed by many references related to this field of research available in other literature. Due to the multidisciplinary nature of this technology, the collection of articles presented here can be used by scientists and researchers in the disciplines of engineering, materials sciences, physics, and chemistry.

InTech Europe
University Campus STeP Ri
Slavka Krautzeka 83/A
51000 Rijeka, Croatia
Phone: +385 (51) 770 447
Fax: +385 (51) 686 166
www.intechopen.com

InTech China
Unit 405, Office Block, Hotel Equatorial Shanghai
No.65, Yan An Road (West), Shanghai, 200040, China
中国上海市延安西路65号上海国际贵都大饭店办公楼405单元
Phone: +86-21-62489820
Fax: +86-21-62489821

IntechOpen